RESULTS FROM CAT AND PROSPECTS FOR THE VSA

Michael E. Jones
Mullard Radio Astronomy Observatory, Cavendish Laboratory, Madingley Road, Cambridge CB3 0HE, UK.

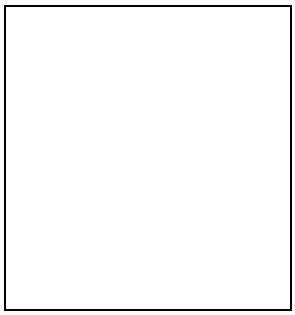

Abstract

We have produced an image of the microwave sky with $30'$ resolution in a 2° field using the Cosmic Anisotropy Telescope (CAT). Analysis of data taken at three frequencies near 15 GHz indicates that most of the signal is due to the CMB, with an equivalent broad-band power of $\Delta T/T = 1.9^{+0.5}_{-0.5} \times 10^{-5}$ at angular scales corresponding to multipoles $l = 320$–500, and $\Delta T/T = 1.8^{+0.7}_{-0.5} \times 10^{-5}$ at $l = 500$–680. We are now building a more advanced instrument, the Very Small Array (VSA), which will cover the range $l = 130$–1800 with a sensitivity per resolution element of $\Delta T/T \sim 10^{-6}$.

1 Introduction

Measurements of the anisotropy in the cosmic microwave background radiation (CMB) in the vicinity of the expected 'Doppler peaks' ($10'$–2°) are crucial for the determination of cosmological parameters such as Ω and H_0, and for discriminating between competing theories of structure formation. Most results on these scales so far have come from balloon-borne switched-beam bolometer systems (eg [1, 2]) or ground-based switched-beam heterodyne systems at dry sites (eg [3, 4]). We have been developing centimetre-wave *interferometers* which offer several advantages over these techniques. These include rejection of groundspill and other signals that do not move with the sky, freedom from $1/f$ noise problems in the receivers, and the rejection of atmospheric emission fluctuations, giving the ability to operate from less extreme sites[5, 6]. The Cosmic Anisotropy Telescope (CAT) is a prototype interferometer designed to test the concepts and technology for a more comprehensive imaging interferometer, the Very Small Array (VSA). In this paper we briefly discuss interferometric imaging of the CMB, review the CAT results and then describe the VSA.

2 Interferometric imaging and power-spectrum estimation

Each antenna pair of an interferometer measures one Fourier component of the part of the sky seen by the envelope (or primary) beam of the antennas, i.e. if a sky brightness distribution $T(\mathbf{s})$ is observed with an interferometer of baseline $\mathbf{u}$ (in wavelengths) then the measured quantity is the *visibility*

$$V(\mathbf{u}) = \frac{2k}{\lambda^2} \int T(\mathbf{s}) B(\mathbf{s}) \mathrm{e}^{i\mathbf{s}.\mathbf{u}} \, \mathrm{d}\mathbf{s}, \tag{1}$$

where $B(\mathbf{s})$ is the power reception pattern (primary beam) of the antennas, and the factor $2k/\lambda^2$ converts from temperature to flux density (the units of an interferometric map being Jy beam^{-1}). Thus a CMB interferometer measures (almost) what the theorist wants to know—$|V(\mathbf{u})|^2$ is proportional to the two-dimensional power spectrum of the sky, but convolved with the square of the Fourier transform of the primary beam. This places a limitation on the resolution with which the power spectrum can be obtained. With a fixed number of antennas of a given aperture, there is a maximum area of aperture plane that can be covered; this fixes the range over which the power spectrum can be measured, or equivalently, the number of resolution elements in the image. A sparsely sampled aperture plane (e.g. the CAT, see Fig. 2) can be inverted to yield a map, but the poor sampling in the aperture leads to long-range correlations in the image. This can be ameliorated by deconvolving the image, using for example the CLEAN algorithm, but such an image must be treated cautiously, since this is equivalent to interpolating the visibilities into regions of the aperture where none were measured. However, a well-sampled aperture plane can be inverted to yield a faithful image of the sky, subject to the resolution limit imposed by the maximum baseline, and the low spatial-frequency cut-off of the shortest baseline.

A image contains both amplitude and phase information; however, if the sky is Gaussian the phases of the Fourier components are random and all the information is contained in the one-dimensional power spectrum. This can naïvely be obtained by averaging the visibilities, first radially into independent bins, then azimuthally, squaring them, and subtracting the variance of the noise from each bin. However, in the case of low signal-to-noise this can result in negative estimates for the power spectrum in some bins. A better method is to calculate the covariance matrix expected of the data under different power-spectrum models, and adopt a maximum-likelihood approach to finding the best model[7, 8].

3 CAT

The CAT[9] is a three-element interferometer operating at 15 GHz, with a primary beam of 2° FWHM and a resolution of $\sim 30'$. The three conical horn-reflector antennas provide a primary beam with sidelobes less than -60 dB, minimising pick-up from the surroundings and from bright astronomical sources. The antennas are steered in elevation by rotating the reflectors, allowing the cryostats containing the HEMT receivers to remain fixed relative to the horn and the turntable, which provides the azimuth drive. The whole telescope is contained within a 5-m-high earth bank lined with aluminium, so that all stray ray paths are reflected on to the sky. The signals are down-converted at the turntable and sent via coaxial cable to a control hut ~ 100 m away, where the 500-MHz-bandwidth IFs are correlated using an analogue phase-switched correlator. Both linear polarizations are used, but the design of the antennas means that the polarization of each channel rotates on the sky as the telescope tracks.

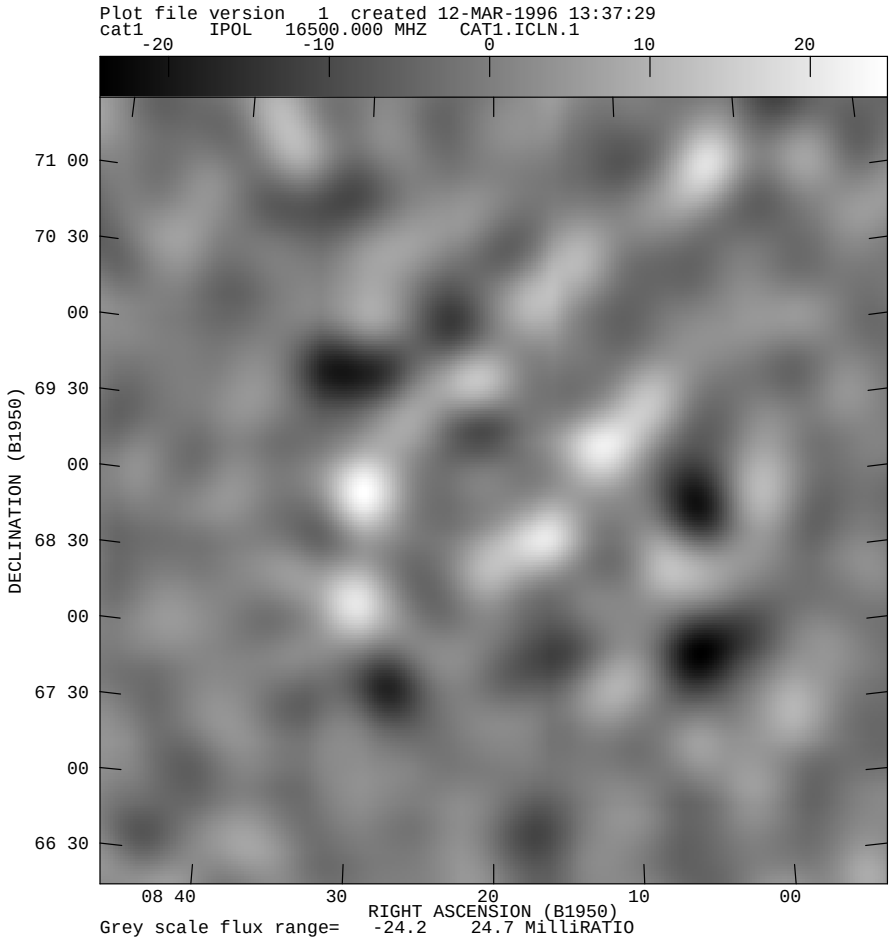

Figure 1: Combined map of 13.5-, 15.5- and 16.5-GHz CAT data, weighted as ν^2 to maximise the CMB component. The map has been CLEANed to remove the long-range correlations due to the sparse sampling of the aperture plane. The greyscale units are mJy beam^{-1}

3.1 Source subtraction

The most important contaminating signal for the CAT is discrete extragalactic radio sources. We select fields at 5 GHz (the highest available frequency with near all-sky coverage) to have minimum source content, but sources still contribute many times the total flux expected from the CMB aniotropies. It is therefore essential to observe these sources at higher flux sensitivity and higher resolution, and at close to the same frequency. This is done using the Ryle Telescope (RT). The RT compact array has five 13-m diameter antennas, giving a flux sensitivity at 15.4 GHz of 200 μJy in 12 h over a $6'$ FWHM field of view, with $30''$ resolution. The flux sensitivity at each of the three CAT frequencies described in the next section is 7 mJy; the RT can map $(0.5^\circ)^2$ with a noise level of 1 mJy in 12 h. Therefore in 16×12 h the RT can map the entire CAT field with sufficient sensitivity to remove all sources to well below the CAT sensitivity.

3.2 CAT results

First results at 13.5 GHz[10] for a field centered at $08^h20^m + 69^\circ$ (B1950) (the 'CAT1' field), showed evidence for a fluctuation level, after subtraction of discrete sources, of 18 mJy beam^{-1}, equivalent to temperature fluctuations of about 35 μK rms. Subsequent observations at 15.5

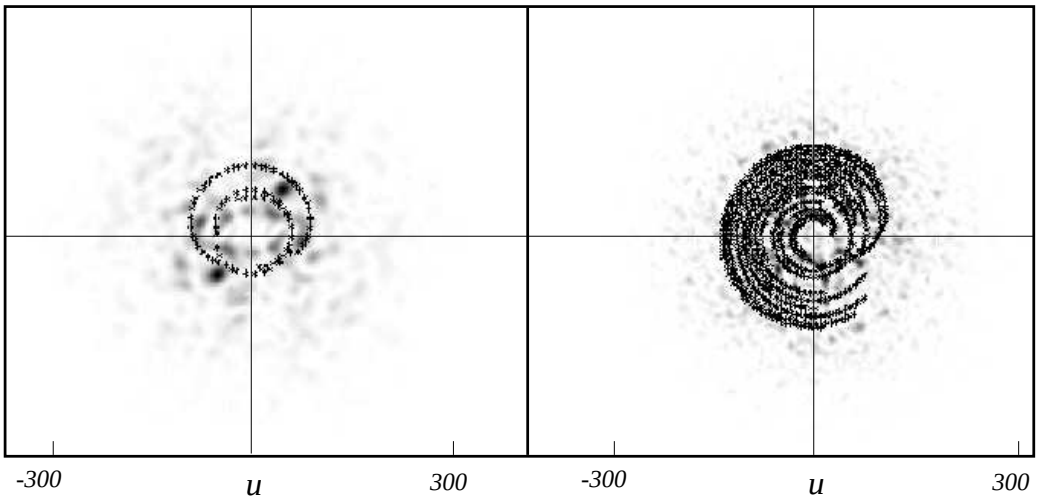

Figure 2: Sample 2-d power spectrum for a standard CDM model, with aperture-plane sampling function of the CAT (left) and the VSA with 4° horns (right). Note the smaller convolution scale of the power spectrum in the case of the VSA due to the larger primary beam.

and 16.5 GHz[8] allow us to estimate the foreground Galactic component and the level of the CMB signal.

The aperture-plane coverage of the CAT results in two independent radial bins, centred at multipole numbers $l = 410$ and $l = 590$. We use a maximum likelihood technique, modelling the CMB and Galactic signals as independent Gaussian signals with variable powers in the two bins, with a fixed flux spectral index of 2 for the CMB and variable in the range $[0, -1]$ for the Galaxy. We then calculate the expected correlation matrix of the visibilities for each model, ranging over the five-dimensional parameter space, and find the maximum likelihood with respect to the data. Marginalising over the Galactic parameters gives the best estimate of the CMB power in the two bins. The data are consistent with most of the signal at 16.5 GHz being due to the microwave background. Taking the square root of the power, the results are $\Delta T/T = 1.9^{+0.5}_{-0.5} \times 10^{-5}$ for the bin covering the range $l = 410 \pm 90$, and $\Delta T/T = 1.8^{+0.7}_{-0.5} \times 10^{-5}$ for the bin at $l = 590 \pm 90$. Given these results, we can combine the three maps at different frequencies, weighted as ν^2, to produce an image that is mostly CMB fluctuations (Fig. 1). This image, unlike the one in [8], has been CLEANed to remove some of the long-range correlations and allow the eye to see more easily the regions of highest and lowest temperature (but note the caveats in section 2 above).

In conjunction with other CMB results, these points provide evidence for the existence of the first Doppler peak, and hence place constraints on the cosmological parameters Ω and H_0 (see Hancock, and Rocha, this volume).

4 The Very Small Array

The CAT is the prototype for the Very Small Array, which is designed to make high-quality images of the CMB. The VSA, which has just received funding (March 1996), will have 15 antennas and a 2-GHz bandwidth analogue correlator, using exactly the same technology as has been successfully tested in the CAT; the specifications are given in Table 1. The operating frequency will be in the range 26–36 GHz, decreasing the effect of discrete sources and Galactic

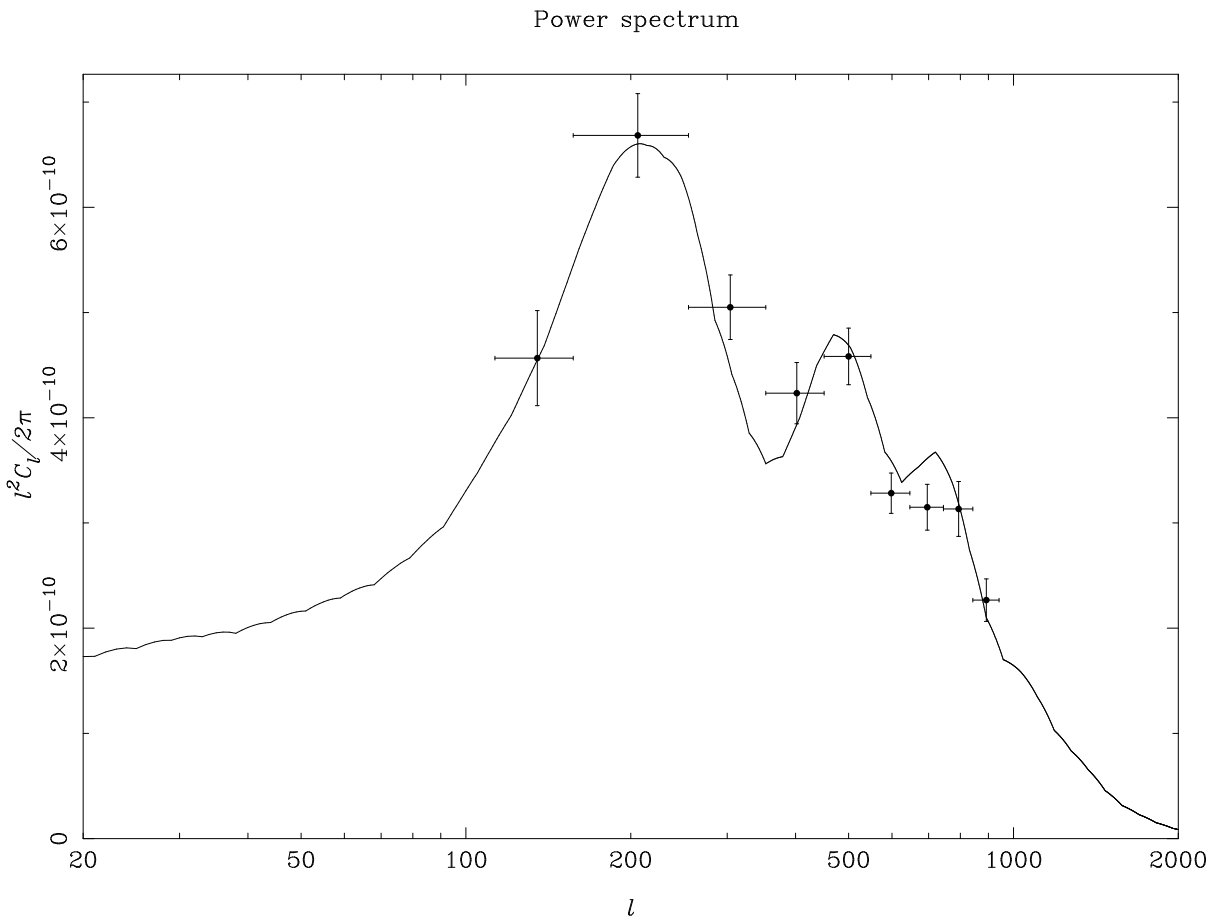

Figure 3: Simulation showing the ability of the VSA to recover the Doppler peaks of the CMB power spectrum. The solid line is a standard CDM power spectrum with $H_0 = 50$, $\Omega_{\rm b} = 0.03$ and $n = 1$, normalised to COBE. The points are the recovered power spectrum from simulated observations of twelve 4° FWHM fields, representing one year's VSA observations. The simulation includes the effects of removal of discrete sources and diffuse galactic foregrounds. The horizontal error bars represent the width of the independent bins sampled in l-space.

emission compared with the CAT frequency range, but increasing the level of atmospheric fluctuation emission. To alleviate the latter effect, the VSA will be sited at the Teide Observatory in Tenerife, alongside the Jodrell Bank–Tenerife switched-beam experiment. Observations with the Tenerife experiment, and a prototype 33-GHz interferometer (R. Watson, priv. comm.) indicate that the atmospheric conditions at Teide will allow the VSA to operate essentially unhindered by the atmosphere for $> 50\%$ of the time.

Source subtraction will be as important for the VSA as for CAT; again, the Ryle Telescope

	Frequency range (GHz)	Number of antennas × polarizations	Field-of -view	Reso-lution	Temperature sensitivity in 300 h	Flux sensitivity in 300 h	Statistical sensitivity
CAT	13.5–16.5	3×2	2°	$30'$	35 μK	7 mJy	9 μK
VSA	26–36	15×1	4(2)°	$30(15)'$	7 μK	5(1.3) mJy	0.7 μK

Table 1: Comparison of specifications of the CAT and the VSA. The temperature sensitivity is per pixel after 300 h observation (as in each of the three CAT maps in [8]). The statistical sensitivity is the temperature sensitivity divided by the square root of the number of independent pixels. Numbers in parentheses for the VSA are for the second array with larger horns.

with its higher resolution and flux sensitivity will be vital. Since the RT observing frequency is a factor of 2 lower than the VSA, the RT will have to survey the VSA fields to a flux sensitivity a factor of 2^α better than the flux sensitivity of the VSA, where α is the maximum expected spectral index of sources in the field. Once all the sources which might be significant at the VSA frequency have been found at 15 GHz, measuring their fluxes at $\sim$ 30 GHz will require only a very short time on a large telescope, e.g. the Bonn 100-m.

The VSA will operate consecutively with two sets of horns; one set of $\sim$ 15 cm aperture giving a 4° beam, and a second set of $\sim$ 30 cm aperture giving a 2° beam. Using the larger horns will allow the VSA to extend to higher angular resolutions without compromising the filling factor of the aperture plane. The CAT, with only three baselines, samples the aperture plane very sparsely, giving only two independent points in the one-dimensional power spectrum. The VSA will measure $\sim$ 100 independent points in the aperture plane, giving $\sim$ 10 independent points on the 1-D power spectrum (see Fig. 3). The width in l of each bin is fixed by the primary beam, i.e. the antenna diameter; the range of l is fixed by the range of baselines possible with 15 antennas and the requirement to sample the aperture plane uniformly. The resolution and range of the measured power spectrum can be changed by changing the size of the antennas. With these two arrays we will be able to measure the power spectrum from $l = 130$–1800 with a resolution $\Delta l = 100$ at low l and $\Delta l = 200$ at high l.

Acknowledgements. Thanks to Mike Hobson and Klaus Maisinger for the VSA power-spectrum simulations. CAT and the VSA are funded by PPARC.

References

[1] Cheng E.S., Cottingham D.A., Fixsen D.J., Inman C.A., Kowitt M.S., Meyer S.S., Page L.A., Puchalla J.L., Ruhl J.E., Silverberg R.F., 1996, *Astrophys. J.* **456**, L71

[2] Clapp A.C., Devlin M.J., Gundersen J.O., Hagmann C.A., Hristov V.V., Lange A.E., Lim M., Lubin P.M., Mauskopf P.D., Meinhold P.R., Richards P. L., Smoot G.F., Tanaka S.T., Timbie P.T., Wuensche C.A., 1994, *Astrophys. J.* **433**, L57

[3] Ruhl J.E., Dragovan M., Platt S.R., Kovac J., Novak G., 1995, *Astrophys. J.* **453**, L1

[4] Netterfield C.B., Jarosik N., Page L., Wilkinson, D., Wollack, E., 1995, *Astrophys. J.* **445**, L69

[5] Saunders R., 1986, in *Highlights of Astronomy* **7**, ed Swings J-P., Reidel

[6] Church S.E., 1995, *MNRAS* **272**, 551

[7] Hobson M.P., Lasenby A.N., Jones M., 1995, *MNRAS* **275**, 863

[8] Scott P.F., Saunders R., Pooley G., O'Sullivan C., Lasenby A.N., Jones M., Hobson M.P., Duffet-Smith P.J., Baker J., 1996, *Astrophys. J.* **461**, L1

[9] Robson M., O'Sullivan C.M., Scott P.F., Duffett-Smith P. J. 1994, *Astr. Astrophys.* **286**, 1028

[10] O'Sullivan C., Yassin G., Woan G., Scott P.F., Saunders R., Robson M., Pooley G., Lasenby A.N., Kenderdine S., Jones M., Hobson M.P., Duffet-Smith P.J., *MNRAS* **274**, 861